Gyrokinetic particle simulations of reversed shear Alfvén eigenmode in nonuniform plasmas with equilibrium current

(author list pending)

Abstract

(abstract pending)

I. INTRODUCTIONS

With the recent electromagnetic upgrade [1], the global gyrokinetic toroidal code (GTC) [2] has been successfully applied to the simulations of the toroidal Alfvén eigenmode (TAE), the reversed shear Alfvén eigenmode (RSAE) [3], and the beta-induced Alfvén eigenmode (BAE) [4]. In the previous formulation [1], the equilibrium current is not considered in the electron continuity equation, and an s-α like (cyclone) magnetic field model is used, in which the equilibrium current effect $\nabla \times \boldsymbol{B}_0 = 0$, because in a lot of cases the equilibrium current effect is not important. We want to recover the $\nabla \times \boldsymbol{B}_0$ terms in the electron continuity equation and to build a field model with self-consistent finite $\nabla \times \boldsymbol{B}_0$ for completeness of the formulation and for the ability to study the cases where finite $\nabla \times \boldsymbol{B}_0$ effect is important. For example, the equilibrium current affects the existence condition for the RSAE [3]. Recovering the equilibrium current will also enable us to simulate the internal kink mode [5]. In this work, only the linear effects are considered. The nonlinear effects will be discussed in a later work.

We start with deriving the electron continuity equation with equilibrium current in Sec. II. To verify the correctness of the derivation, we show that the GTC formulation reduces to the ideal MHD theory in certain limits in Sec. III. For code implementation, the electron continuity equation with current is expressed in magnetic coordinates and normalized in Sec. IV. Then the field model with finite $\nabla \times \boldsymbol{B}_0$ is derived Sec. V. The equilibrium current effect on RSAE is discussed with analytic calculation and simulation results in Sec. VI. Finally, simulations of a real experiment, the DIII-D discharge #142111 at 750ms, are presented in Sec. VII.

II. ELECTRON CONTINUITY EQUATION BY INTEGRATING DRIFT-KINETIC EQUATION

This section is to extend the electron contiuity equation Eq. (10) of Ref. [1] to include equilibrium current and finite $\nabla \times \boldsymbol{B}_0$. The drift-kinetic equation with quantities decomposed into equilibrium and perturbed components writes:

$$(\partial_t + \dot{\boldsymbol{X}}\cdot\nabla + \dot{v}_\parallel \partial_{v_\parallel})[f_0(\boldsymbol{X},\mu,v_\parallel) + \delta f(\boldsymbol{X},\mu,v_\parallel,t)] = 0 \;, \tag{1}$$

$$\dot{\boldsymbol{X}} = v_\parallel \frac{\boldsymbol{B}_0 + \delta\boldsymbol{B}}{B_0} + \underbrace{\frac{c\boldsymbol{b}_0\times\nabla\phi}{B_0}}_{\boldsymbol{v}_E} + \underbrace{\frac{v_\parallel^2}{\Omega}\nabla\times\boldsymbol{b}_0}_{\boldsymbol{v}_c} + \underbrace{\frac{\mu}{m\Omega}\boldsymbol{b}_0\times\nabla B_0}_{\boldsymbol{v}_g} \;, \tag{2}$$

$$\dot{v}_\parallel = -\frac{1}{m}\frac{\boldsymbol{B}_0 + \frac{B_0 v_\parallel}{\Omega}\nabla\times\boldsymbol{b}_0 + \delta\boldsymbol{B}}{B_0}\cdot(\mu\nabla B_0 + Z\nabla\phi) - \frac{Z}{mc}\partial_t A_\parallel \;. \tag{3}$$

Assuming no equilibrium electric field ($\phi_0 = 0$), and the equilibrium magnetic field is time-independent ($\partial_t A_{\parallel 0} = 0$), we can make such substitutions:

$$\phi \to \delta\phi \;, \qquad \partial_t A_\parallel \to \partial_t\, \delta A_\parallel \;, \tag{4}$$

Integrating Eq. (1) over the guiding center velocity space:

$$\int_{\mathrm{GC}} \mathrm{d}\boldsymbol{v} = \frac{2\pi B_0}{m}\int \mathrm{d}\mu \mathrm{d}v_\parallel \;, \tag{5}$$

we get an equilibrium equation:

$$\boldsymbol{B}_0\cdot\nabla\left(\frac{n_0 u_{\parallel 0}}{B_0}\right) + \frac{c\nabla\times\boldsymbol{b}_0}{Z}\cdot\nabla\left(\frac{P_{\parallel 0}}{B_0}\right) + \frac{c\boldsymbol{b}_0\times\nabla B_0}{Z}\cdot\nabla\left(\frac{P_{\perp 0}}{B_0^2}\right) + \frac{c\nabla\times\boldsymbol{b}_0\cdot\nabla B_0}{ZB_0^2}P_{\perp 0} = 0 \;, \tag{6}$$

and an linear equation:

$$\begin{aligned}
0 &= \partial_t\,\delta n + \delta\boldsymbol{B}\cdot\nabla\left(\frac{n_0 u_{\parallel 0}}{B_0}\right) + B_0\boldsymbol{v}_E\cdot\nabla\left(\frac{n_0}{B_0}\right) + \boldsymbol{B}_0\cdot\nabla\left(\frac{n_0\,\delta u_\parallel}{B_0}\right) \\
&\quad + \frac{c\nabla\times\boldsymbol{b}_0}{Z}\cdot\nabla\left(\frac{\delta P_\parallel}{B_0}\right) + \frac{c\boldsymbol{b}_0\times\nabla B_0}{Z}\cdot\nabla\left(\frac{\delta P_\perp}{B_0^2}\right) + \frac{c\nabla\times\boldsymbol{b}_0\cdot\nabla B_0}{ZB_0^2}\,\delta P_\perp \\
&\quad + \frac{c\nabla\times\boldsymbol{b}_0}{B_0}\cdot n_0\nabla\,\delta\phi \qquad (7)\\
&= \partial_t\,\delta n + \delta\boldsymbol{B}\cdot\nabla\left(\frac{n_0 u_{\parallel 0}}{B_0}\right) + \boldsymbol{B}_0\cdot\nabla\left(\frac{n_0\,\delta u_\parallel}{B_0}\right) + B_0\boldsymbol{v}_E\cdot\nabla\left(\frac{n_0}{B_0}\right) \\
&\quad - n_0(\delta\boldsymbol{v}_* + \boldsymbol{v}_E)\cdot\frac{\nabla B_0}{B_0} + \frac{c\nabla\times\boldsymbol{B}_0}{ZB_0^2}\cdot\nabla\,\delta P_\parallel + \frac{c\nabla\times\boldsymbol{B}_0\cdot\nabla B_0}{ZB_0^3}(\delta P_\perp - \delta P_\parallel) \\
&\quad + n_0\frac{c\nabla\times\boldsymbol{B}_0}{B_0^2}\cdot\nabla\,\delta\phi \;, \qquad (8)
\end{aligned}$$

where

$$\delta\boldsymbol{v}_* = \frac{c}{n_0 Z B_0}\boldsymbol{b}_0\times\nabla(\delta P_\perp + \delta P_\parallel) \tag{9}$$

is the perturbed diamagnetic drift. Apply this equation to the electrons ($Z_e = -e$):

$$
\begin{aligned}
0 &= \partial_t\, \delta n_e + \delta \boldsymbol{B} \cdot \nabla \left(\frac{n_{0e} u_{\parallel 0e}}{B_0} \right) + B_0 \boldsymbol{v}_E \cdot \nabla \left(\frac{n_{0e}}{B_0} \right) + \boldsymbol{B}_0 \cdot \nabla \left(\frac{n_{0e}\, \delta u_{\parallel e}}{B_0} \right) \\
&\quad - \frac{c \nabla \times \boldsymbol{b}_0}{e} \cdot \nabla \left(\frac{\delta P_{\parallel e}}{B_0} \right) - \frac{c \boldsymbol{b}_0 \times \nabla B_0}{e} \cdot \nabla \left(\frac{\delta P_{\perp e}}{B_0^2} \right) - \frac{c \nabla \times \boldsymbol{b}_0 \cdot \nabla B_0}{e B_0^2}\, \delta P_{\perp e} \\
&\quad + \frac{c \nabla \times \boldsymbol{b}_0}{B_0} \cdot n_{0e} \nabla\, \delta\phi \qquad (10) \\
&= \partial_t\, \delta n_e + \delta \boldsymbol{B} \cdot \nabla \left(\frac{n_{0e} u_{\parallel 0e}}{B_0} \right) + \boldsymbol{B}_0 \cdot \nabla \left(\frac{n_{0e}\, \delta u_{\parallel e}}{B_0} \right) + B_0 \boldsymbol{v}_E \cdot \nabla \left(\frac{n_{0e}}{B_0} \right) \\
&\quad - n_{0e} (\delta \boldsymbol{v}_{*e} + \boldsymbol{v}_E) \cdot \frac{\nabla B_0}{B_0} \\
&\quad + \frac{c \nabla \times \boldsymbol{B}_0}{B_0^2} \cdot \left[- \frac{\nabla\, \delta P_{\parallel e}}{e} - \frac{(\delta P_{\perp e} - \delta P_{\parallel e}) \nabla B_0}{e B_0} + n_{0e} \nabla\, \delta\phi \right] . \qquad (11)
\end{aligned}
$$

The second and the last term in Eq. (8) are new terms introduced by the equilibrium current and finite $\nabla \times \boldsymbol{B}_0$. Other terms are identical to those in Eq. (10) of Ref. [1].

III. REDUCTION OF GYROKINETIC FORMULATION TO IDEAL MHD

In this section, we prove that with appropriate approximations, the gyrokinetic formulation [1] reduces to the ideal MHD theory [6].

A. Reduction of the field equations

Gyrokinetic Poisson's equation [7] with two ion species:

$$
\frac{Z_i^2 n_i}{T_i} (\delta\phi - \delta\tilde{\phi}_i) + \frac{Z_f^2 n_f}{T_f} (\delta\phi - \delta\tilde{\phi}_f) = \sum_{\alpha = i,f,e} Z_\alpha \delta n_\alpha \ , \qquad (12)
$$

where for the ion species ($\alpha = i, f$) [8],

$$
\begin{aligned}
\delta\tilde{\phi}_\alpha(\boldsymbol{x}, t) &= \frac{1}{n_\alpha} \int_{\boldsymbol{X} \to \boldsymbol{x}} \mathrm{d}\boldsymbol{v}\, f_\alpha(\boldsymbol{X}, \mu, v_\parallel, t) \left\langle \delta\phi \right\rangle (\boldsymbol{X}, t) \ , \qquad (13) \\
\delta n_\alpha(\boldsymbol{x}, t) &= \int_{\boldsymbol{X} \to \boldsymbol{x}} \mathrm{d}\boldsymbol{v}\, \delta f_\alpha(\boldsymbol{X}, \mu, v_\parallel, t) \ , \qquad (14)
\end{aligned}
$$

and the integral symbol here is short for the integral over the guiding center velocity space and the transformation between the guiding center and the particle coordinates:

$$
\int_{\boldsymbol{X} \to \boldsymbol{x}} \mathrm{d}\boldsymbol{v} \equiv \int \frac{2\pi B_0}{m} \mathrm{d}\mu \mathrm{d}v_\parallel \int \frac{\mathrm{d}\vartheta_c}{2\pi} \mathrm{d}\boldsymbol{X}\, \delta(\boldsymbol{X} + \boldsymbol{\rho} - \boldsymbol{x}) \ , \qquad (15)
$$

and ϑ_c is the gyro-phase angle. From Eq. (15) it can be seen that the first part of the integral, which is over the guiding center velocity space, is the same as $\int_{\mathrm{GC}} \mathrm{d}\boldsymbol{v}$ defined in Eq. (5). The second part of the integral, which is the transformation between the guiding center coordinates and the particle coordinates, gives an operator $\mathfrak{J}_0(k_\perp \rho)$, where $\mathfrak{J}_0()$ is the Bessel function. In the GTC, this $\mathfrak{J}_0(k_\perp \rho)$ is reflected in the charge scattering from each particle's guiding center to its gyro-orbit when collecting charges from the particles. Note that the gyro-averaging on the perturbed field quantities also gives an operator $\mathfrak{J}_0(k_\perp \rho)$:

$$\langle \delta\phi \rangle = \mathfrak{J}_0(k_\perp \rho)\, \delta\phi \ . \tag{16}$$

In the case of $k_\perp \rho_{i,f} < 1$, we can expand the $\mathfrak{J}_0^2$ operator and keep terms up to $O(k_\perp^2 \rho^2)$.

$$\begin{aligned}
\mathfrak{J}_0^2(k_\perp \rho_\alpha) &= \mathfrak{J}_0^2\left(k_\perp \frac{\sqrt{2\mu B_0/m_\alpha}}{\Omega_\alpha}\right) \\
&\approx 1 - \frac{\mu m_\alpha c^2}{Z_\alpha^2 B_0} k_\perp^2 \\
&= 1 + \frac{\mu m_\alpha c^2}{Z_\alpha^2 B_0} \nabla_\perp^2
\end{aligned} \tag{17}$$

Assume that the equilibrium distribution is a shifted Maxwellian for both ion species:

$$f_{0\alpha} = \frac{n_{0\alpha}}{(2\pi v_{th,\alpha})^{3/2}} \exp\left[\frac{-(v_\parallel - u_{\parallel 0\alpha})^2 - \frac{2\mu B_0}{m_\alpha}}{2 v_{th,\alpha}^2}\right] \qquad \alpha = i, f \ , \tag{18}$$

where $v_{th,\alpha} = \sqrt{T_\alpha / m_\alpha}$ is the ion thermal velocity. Then in the linear limit, $\delta\tilde{\phi}_\alpha$ becomes:

$$\begin{aligned}
\delta\tilde{\phi}_\alpha &= \frac{1}{n_{0\alpha}} \int_{\mathrm{GC}} \mathrm{d}\boldsymbol{v}\, \mathfrak{J}_0^2(k_\perp \rho_\alpha)\, \delta\phi f_{0\alpha} \\
&\approx \frac{1}{n_{0\alpha}} \int_{\mathrm{GC}} \mathrm{d}\boldsymbol{v}\, f_{0\alpha} \left(1 + \frac{\mu m_\alpha c^2}{Z_\alpha^2 B_0} \nabla_\perp^2\right) \delta\phi \\
&= \delta\phi + \frac{m_\alpha c^2 T_\alpha}{Z_i^2 B_0^2} \nabla_\perp^2\, \delta\phi
\end{aligned} \tag{19}$$

Then Eq. (12) reduces to:

$$\begin{aligned}
&\sum_{\alpha = i,f,e} Z_\alpha\, \delta n_\alpha \\
&= \frac{Z_i^2 n_i}{T_i} (\delta\phi - \delta\tilde{\phi}_i) + \frac{Z_f^2 n_f}{T_f} (\delta\phi - \delta\tilde{\phi}_f) \\
&\approx -\frac{(n_{0i} m_i + n_{0f} m_f) c^2}{B_0^2} \nabla_\perp^2\, \delta\phi \\
&= -\frac{c^2}{4\pi v_A^2} \nabla_\perp^2\, \delta\phi \ ,
\end{aligned} \tag{20}$$

where

$$v_A^2 = \frac{B_0^2}{4\pi(n_{i0}m_i + n_{f0}m_f)} \ . \tag{21}$$

Note that if the fast ion distribution is not a (shifted) Maxwellian and its density is comparable to the thermal ion density, this reduction may not be valid.

The parallel gyrokinetic Ampère's law writes:

$$\frac{c}{4\pi}\boldsymbol{b}_0 \cdot \nabla \times [\nabla \times (\delta A_\parallel \boldsymbol{b}_0)]\boldsymbol{b}_0 = \sum_{\alpha=i,f,e} \delta \boldsymbol{J}_{\parallel\alpha} \ , \tag{22}$$

where the vector potential has only the parallel component $\delta A_\parallel$ ($\delta B_\parallel = 0$ limit), and

$$\delta J_{\parallel\alpha}(\boldsymbol{x}, t) = \int_{\boldsymbol{X}\to\boldsymbol{x}} \mathrm{d}\boldsymbol{v}\, Z_\alpha v_\parallel\, \delta f_\alpha(\boldsymbol{X}, \mu, v_\parallel, t) \qquad \alpha = i, f \ . \tag{23}$$

For electrons, the particle position and the guiding center position are not distinguished because of their small gyro-radii ($k_\perp \rho_e \ll 1$), so their density and current are simply just:

$$\delta n_e = \int_{\mathrm{GC}} \mathrm{d}\boldsymbol{v}\, \delta f_e \ , \tag{24}$$

$$\delta J_{\parallel e} = -e \int_{\mathrm{GC}} \mathrm{d}\boldsymbol{v}\, v_\parallel\, \delta f_e \ , \tag{25}$$

which are described by the electron continuity equation Eq. (11).

In the ideal MHD limit, $\delta E_\parallel = 0$, and as a result:

$$\partial_t\, \delta A_\parallel = -c\boldsymbol{b}_0 \cdot \nabla\, \delta\phi \ . \tag{26}$$

Combine Eq. (20), Eq. (22), and Eq. (26) and take the linear normal mode theory substitution $\partial_t \to -i\omega$ and $\boldsymbol{b}_0 \cdot \nabla \to ik_\parallel$ to get the reduced field equation:

$$\begin{aligned} \frac{\omega^2}{v_A^2}\nabla_\perp^2\, \delta\phi - i\boldsymbol{B}_0 \cdot \nabla \left\{ \frac{\boldsymbol{b}_0 \cdot \nabla \times [\nabla \times (k_\parallel\, \delta\phi \boldsymbol{b}_0)]}{B_0} \right\} & \\ + i\omega \frac{4\pi}{c^2} \sum_\alpha (-i\omega Z_\alpha\, \delta n_\alpha + \nabla \cdot \delta \boldsymbol{J}_{\parallel\alpha}) = 0 \ . & \end{aligned} \tag{27}$$

B. Reduction of the ion equation

To obtain an equation describing δn_α and $\delta J_{\parallel\alpha}$ for both ion species ($\alpha = i, f$), we operate $\int_{\boldsymbol{X}\to\boldsymbol{x}} \mathrm{d}\boldsymbol{v}$ on the gyrokinetic equation, which is used to describe the ions in the GTC. The gyrokinetic equation is the same as the drift-kinetic equation Eq. (1), except that the field quantities are gyro-averaged in the gyrokinetic equation:

$$
(\partial_t + \dot{\boldsymbol{X}} \cdot \nabla + \dot{v}_\parallel \partial_{v_\parallel})[f_0(\boldsymbol{X}, \mu, v_\parallel) + \delta f(\boldsymbol{X}, \mu, v_\parallel, t)] = 0 \ , \tag{28}
$$

$$
\dot{\boldsymbol{X}} = v_\parallel \frac{\boldsymbol{B}_0 + \langle \delta \boldsymbol{B} \rangle}{B_0} + \underbrace{\frac{c\boldsymbol{b}_0 \times \nabla \langle \delta\phi \rangle}{B_0}}_{\langle \boldsymbol{v}_E \rangle} + \underbrace{\frac{v_\parallel^2}{\Omega} \nabla \times \boldsymbol{b}_0}_{\boldsymbol{v}_c} + \underbrace{\frac{\mu}{m\Omega} \boldsymbol{b}_0 \times \nabla B_0}_{\boldsymbol{v}_g} \ , \tag{29}
$$

$$
\dot{v}_\parallel = -\frac{1}{m} \frac{\boldsymbol{B}_0 + \frac{B_0 v_\parallel}{\Omega} \nabla \times \boldsymbol{b}_0 + \langle \delta \boldsymbol{B} \rangle}{B_0} \cdot (\mu \nabla B_0 + Z \nabla \langle \delta\phi \rangle) - \frac{Z}{mc} \partial_t \left\langle \delta A_\parallel \right\rangle \ . \tag{30}
$$

Similar to Eq. (16), the gyro-averaging gives a $\mathfrak{J}_0(k_\perp \rho)$ operator:

$$
\langle \delta \boldsymbol{B} \rangle = \mathfrak{J}_0(k_\perp \rho) \, \delta \boldsymbol{B} \ , \tag{31}
$$

$$
\left\langle \delta A_\parallel \right\rangle = \mathfrak{J}_0(k_\perp \rho) \, \delta A_\parallel \ . \tag{32}
$$

Integrating the gyrokinetic equation in the linear limit gives:

$$
\begin{aligned}
0 =& \int_{\boldsymbol{X} \to \boldsymbol{x}} \mathrm{d}\boldsymbol{v} \, (\partial_t + \dot{\boldsymbol{X}} \cdot \nabla + \dot{v}_\parallel \partial_{v_\parallel})(f_{0\alpha} + \delta f_\alpha) \\
=& \, \boldsymbol{B}_0 \cdot \nabla \left(\frac{n_{0\alpha} u_{\parallel 0\alpha}}{B_0} \right) + \frac{c \nabla \times \boldsymbol{b}_0}{Z_\alpha} \cdot \nabla \left(\frac{P_{\parallel 0\alpha}}{B_0} \right) + \frac{c\boldsymbol{b}_0 \times \nabla B_0}{Z_\alpha} \cdot \nabla \left(\frac{P_{\perp 0\alpha}}{B_0^2} \right) + \frac{c \nabla \times \boldsymbol{b}_0 \cdot \nabla B_0}{Z_\alpha B_0^2} P_{\perp 0\alpha} \\
& + \partial_t \, \delta n_\alpha + \delta \boldsymbol{B} \cdot \nabla \left(\frac{n_{0\alpha} u_{\parallel 0\alpha}}{B_0} \right) + B_0 \boldsymbol{v}_E \cdot \nabla \left(\frac{n_{0\alpha}}{B_0} \right) + \boldsymbol{B}_0 \cdot \nabla \left(\frac{n_{0\alpha} \, \delta u_{\parallel\alpha}}{B_0} \right) \\
& + \frac{c \nabla \times \boldsymbol{b}_0}{Z_\alpha} \cdot \nabla \left(\frac{\delta P_{\parallel\alpha}}{B_0} \right) + \frac{c\boldsymbol{b}_0 \times \nabla B_0}{Z_\alpha} \cdot \nabla \left(\frac{\delta P_{\perp\alpha}}{B_0^2} \right) + \frac{c \nabla \times \boldsymbol{b}_0 \cdot \nabla B_0}{Z_\alpha B_0^2} \, \delta P_{\perp\alpha} \\
& + \frac{c \nabla \times \boldsymbol{b}_0}{B_0} \cdot n_{0\alpha} \nabla \, \delta\phi + \frac{m_\alpha c^2}{Z_\alpha^2 B_0} (\nabla_\perp^2 \, \delta \boldsymbol{B}) \cdot \nabla \left(\frac{P_{0\alpha} u_{\parallel 0\alpha}}{B_0^2} \right) - \frac{m_\alpha c^3 \boldsymbol{b}_0 \times \nabla P_{0\alpha}}{Z_\alpha^2 B_0^2} \cdot \nabla \frac{\nabla_\perp^2 \, \delta\phi}{B_0} \\
& + \frac{m_\alpha c^3 P_{0\alpha} (3\boldsymbol{b}_0 \times \nabla B_0 + \nabla \times \boldsymbol{B}_0)}{Z_\alpha^2 B_0^3} \cdot \nabla \frac{\nabla_\perp^2 \, \delta\phi}{B_0} \ .
\end{aligned} \tag{33}
$$

This equation can be separated into the equilibrium equation:

$$
\boldsymbol{B}_0 \cdot \nabla \left(\frac{n_{0\alpha} u_{\parallel 0\alpha}}{B_0} \right) + \frac{c \nabla \times \boldsymbol{b}_0}{Z_\alpha} \cdot \nabla \left(\frac{P_{\parallel 0\alpha}}{B_0} \right) + \frac{c\boldsymbol{b}_0 \times \nabla B_0}{Z_\alpha} \cdot \nabla \left(\frac{P_{\perp 0\alpha}}{B_0^2} \right) + \frac{c \nabla \times \boldsymbol{b}_0 \cdot \nabla B_0}{Z_\alpha B_0^2} P_{\perp 0\alpha} = 0 \ , \tag{34}
$$

and the linear equation:

$$
\begin{aligned}
0 = {} & \partial_t \, \delta n_\alpha + \delta \boldsymbol{B} \cdot \nabla \left(\frac{n_{0\alpha} u_{\parallel 0\alpha}}{B_0} \right) + B_0 \boldsymbol{v}_E \cdot \nabla \left(\frac{n_{0\alpha}}{B_0} \right) + \boldsymbol{B}_0 \cdot \nabla \left(\frac{n_{0\alpha} \, \delta u_{\parallel\alpha}}{B_0} \right) \\
& + \frac{c \nabla \times \boldsymbol{b}_0}{Z_\alpha} \cdot \nabla \left(\frac{\delta P_{\parallel\alpha}}{B_0} \right) + \frac{c \boldsymbol{b}_0 \times \nabla B_0}{Z_\alpha} \cdot \nabla \left(\frac{\delta P_{\perp\alpha}}{B_0^2} \right) + \frac{c \nabla \times \boldsymbol{b}_0 \cdot \nabla B_0}{Z_\alpha B_0^2} \, \delta P_{\perp\alpha} \\
& + \frac{c \nabla \times \boldsymbol{b}_0}{B_0} \cdot n_{0\alpha} \nabla \, \delta\phi \underbrace{+ \frac{m_\alpha c^2}{Z_\alpha^2 B_0} (\nabla_\perp^2 \, \delta \boldsymbol{B}) \cdot \nabla \left(\frac{P_{0\alpha} u_{\parallel 0\alpha}}{B_0^2} \right)}_{\{i\}} \underbrace{- \frac{m_\alpha c^3 \boldsymbol{b}_0 \times \nabla P_{0\alpha}}{Z_\alpha^2 B_0^2} \cdot \nabla \frac{\nabla_\perp^2 \, \delta\phi}{B_0}}_{\{ii\}} \\
& \underbrace{+ \frac{m_\alpha c^3 P_{0\alpha} (3 \boldsymbol{b}_0 \times \nabla B_0 + \nabla \times \boldsymbol{B}_0)}{Z_\alpha^2 B_0^3} \cdot \nabla \frac{\nabla_\perp^2 \, \delta\phi}{B_0}}_{\{iii\}} \, .
\end{aligned} \tag{35}
$$

These two equations are the same as those of the electrons Eqs. (6) and (8) except for the last three terms in Eq. (35), which are introduced by the ion finite Larmor radius (FLR) effects. In the $k_\perp L_{B_0} \sim k_\perp R_0 \gg 1$ limit, the term $\{ii\}$ becomes:

$$
\begin{aligned}
\{ii\} & \approx - \frac{m_\alpha c^2 n_{0\alpha}}{Z_\alpha B_0^2} \frac{c \boldsymbol{b}_0 \times \nabla P_{0\alpha}}{Z_\alpha B_0 n_{0\alpha}} \cdot \nabla \nabla_\perp^2 \, \delta\phi \\
& = - \frac{m_\alpha c^2 n_{0\alpha}}{Z_\alpha B_0^2} \boldsymbol{v}_{*\alpha} \cdot \nabla \nabla_\perp^2 \, \delta\phi \, ,
\end{aligned} \tag{36}
$$

where

$$
\boldsymbol{v}_{*\alpha} = \frac{c \boldsymbol{b}_0 \times \nabla P_{0\alpha}}{Z_\alpha B_0 n_{0\alpha}} \, . \tag{37}
$$

For the thermal ion species, this term is responsible for producing the kinetic ballooning mode [9]. We compare the ordering of this term with the other two FLR terms:

$$
O\left(\frac{\{iii\}}{\{ii\}} \right) \sim \frac{L_{P_{0\alpha}}}{L_{B_0}} \, , \tag{38}
$$

$$
O\left(\frac{\{i\}}{\{ii\}} \right) \sim \frac{k_\parallel u_{\parallel 0\alpha}}{\omega} \left(1 + \frac{L_{P_{0\alpha}}}{L_{u_{\parallel 0\alpha}}} - 2 \frac{L_{P_{0\alpha}}}{L_{B_0}} \right) \, . \tag{39}
$$

In the case of $L_{P_{0\alpha}} < L_{B_0}$, $L_{P_{0\alpha}} \lesssim L_{u_{\parallel 0\alpha}}$, and $k_\parallel u_{\parallel 0\alpha} \ll \omega$, the terms $\{i\}$ and $\{iii\}$ are not important and can be dropped. Keeping term $\{ii\}$ as the only FLR effect, the ion continuity equation reforms to be:

$$
\begin{aligned}
& Z_\alpha \partial_t \, \delta n_\alpha + \boldsymbol{B}_0 \cdot \nabla \left(\frac{Z_\alpha n_{0\alpha} \, \delta u_{\|\alpha}}{B_0} \right) \\
= & -i\omega Z_\alpha \, \delta n_\alpha + \nabla \cdot \delta \boldsymbol{J}_{\|\alpha} \\
\approx & -\delta \boldsymbol{B} \cdot \nabla \left(\frac{J_{\|0\alpha}}{B_0} \right) - B_0 \boldsymbol{v}_E \cdot \nabla \left(\frac{Z_\alpha n_{0\alpha}}{B_0} \right) + \frac{m_\alpha c^2 n_{0\alpha}}{B_0^2} \boldsymbol{v}_{*\alpha} \cdot \nabla \nabla_\perp^2 \, \delta\phi \\
& -c\nabla \times \boldsymbol{b}_0 \cdot \nabla \left(\frac{\delta P_{\|\alpha}}{B_0} \right) - c\boldsymbol{b}_0 \times \nabla B_0 \cdot \nabla \left(\frac{\delta P_{\perp\alpha}}{B_0^2} \right) - \frac{c\nabla \times \boldsymbol{b}_0 \cdot \nabla B_0}{B_0^2} \, \delta P_{\perp\alpha} \\
& -\frac{c\nabla \times \boldsymbol{b}_0}{B_0} \cdot Z_\alpha n_{0\alpha} \nabla \, \delta\phi \ .
\end{aligned} \tag{40}
$$

C. Combine the reduced equations

The electron continuity equation Eq. (10) reforms to be:

$$
\begin{aligned}
& -e\partial_t \, \delta n_e - \boldsymbol{B}_0 \cdot \nabla \left(\frac{e n_{\alpha 0} \, \delta u_{\alpha\|}}{B_0} \right) \\
= & \, i\omega e \, \delta n_e + \nabla \cdot \delta \boldsymbol{J}_{\|e} \\
= & -\delta \boldsymbol{B} \cdot \nabla \left(\frac{J_{\|0e}}{B_0} \right) + B_0 \boldsymbol{v}_E \cdot \nabla \left(\frac{e n_{0e}}{B_0} \right) \\
& -c\nabla \times \boldsymbol{b}_0 \cdot \nabla \left(\frac{\delta P_{\|e}}{B_0} \right) - c\boldsymbol{b}_0 \times \nabla B_0 \cdot \nabla \left(\frac{\delta P_{\perp e}}{B_0^2} \right) - \frac{c\nabla \times \boldsymbol{b}_0 \cdot \nabla B_0}{B_0^2} \, \delta P_{\perp e} \\
& +\frac{c\nabla \times \boldsymbol{b}_0}{B_0} \cdot e n_{0e} \nabla \, \delta\phi \ .
\end{aligned} \tag{41}
$$

Plug Eqs. (41) and (40) into Eq. (27), and consider Eq. (21), quasi-neutrality $\sum_\alpha Z_\alpha n_{\alpha 0} = 0$ and Ampère's law for equilibrium $\sum_\alpha J_{\alpha\|0} = \frac{c}{4\pi} \boldsymbol{b}_0 \cdot \nabla \times \boldsymbol{B}_0$, we get:

$$
\begin{aligned}
0 = & \frac{\omega(\omega - \omega_{*P})}{v_A^2} \nabla_\perp^2 \, \delta\phi - i\boldsymbol{B}_0 \cdot \nabla \left\{ \frac{\boldsymbol{b}_0 \cdot \nabla \times [\nabla \times (k_\| \, \delta\phi \boldsymbol{b}_0)]}{B_0} \right\} \\
& -\frac{i\omega}{c} \delta \boldsymbol{B} \cdot \nabla \left(\frac{\boldsymbol{b}_0 \cdot \nabla \times \boldsymbol{B}_0}{B_0} \right) \\
& -i\omega \frac{4\pi}{c} \left[\nabla \times \boldsymbol{b}_0 \cdot \nabla \left(\frac{\delta P_\|}{B_0} \right) + \boldsymbol{b}_0 \times \nabla B_0 \cdot \nabla \left(\frac{\delta P_\perp}{B_0^2} \right) + \frac{\nabla \times \boldsymbol{b}_0 \cdot \nabla B_0}{B_0^2} \, \delta P_\perp \right] \ ,
\end{aligned} \tag{42}
$$

where $\delta P_\| = \sum_\alpha \delta P_{\alpha\|}$, $\delta P_\perp = \sum_\alpha \delta P_{\alpha\perp}$, and

$$
\omega_{*P} = -i\boldsymbol{v}_* \cdot \nabla \ , \tag{43}
$$

$$
\boldsymbol{v}_* = \frac{n_{0i} m_i \boldsymbol{v}_{*i} + n_{0f} m_f \boldsymbol{v}_{*f}}{n_{0i} m_i + n_{0f} m_f} \ . \tag{44}
$$

Now the first three terms of Eq. (42) match those of the MHD equation [6]. The last term, i.e., the pressure term, needs more analysis.

D. The pressure term mismatch is negligible

For comparison convenience, we write down the pressure terms (with the $-i\omega 4\pi/c$ coefficients removed) from the two different approaches:

$$\mathrm{PT}_{\mathrm{MHD}} = \nabla\cdot\left(\frac{\boldsymbol{b}_0}{B_0}\times\nabla\cdot\delta\mathbb{P}\right) \ , \tag{45}$$

$$\begin{aligned}\mathrm{PT}_{\mathrm{GK}} &= \nabla\times\boldsymbol{b}_0\cdot\nabla\left(\frac{\delta P_\parallel}{B_0}\right)+\boldsymbol{b}_0\times\nabla B_0\cdot\nabla\left(\frac{\delta P_\perp}{B_0^2}\right)+\frac{\nabla\times\boldsymbol{b}_0\cdot\nabla B_0}{B_0^2}\,\delta P_\perp\\ &= \frac{\boldsymbol{b}_0\times\nabla B_0}{B_0^2}\cdot\nabla(\delta P_\perp+\delta P_\parallel)+\frac{\nabla\times\boldsymbol{B}_0}{B_0^2}\cdot\nabla\delta P_\parallel\\ &\quad+\frac{\nabla\times\boldsymbol{B}_0\cdot\nabla B_0}{B_0^3}(\delta P_\perp-\delta P_\parallel)\ .\end{aligned} \tag{46}$$

Assume $\delta\mathbb{P}$ is diagonal:

$$\begin{aligned}\delta\mathbb{P} &= \delta P_\parallel\boldsymbol{b}_0\boldsymbol{b}_0+\delta P_\perp(\mathbb{I}-\boldsymbol{b}_0\boldsymbol{b}_0)\\ &= \delta P_\perp\mathbb{I}+(\delta P_\parallel-\delta P_\perp)\boldsymbol{b}_0\boldsymbol{b}_0\ .\end{aligned} \tag{47}$$

Then we have:

$$\begin{aligned}\mathrm{PT}_{\mathrm{MHD}} = &\frac{\nabla\times\boldsymbol{B}_0+\boldsymbol{b}_0\times\nabla B_0}{B_0^2}\cdot\nabla\,\delta P_\perp+\frac{\boldsymbol{b}_0\times\nabla B_0}{B_0^2}\cdot\nabla\,\delta P_\parallel+\frac{(\nabla\times\boldsymbol{B}_0)_\perp}{B_0}\cdot\nabla\left(\frac{\delta P_\parallel-\delta P_\perp}{B_0}\right)\\ &+\frac{\delta P_\parallel-\delta P_\perp}{B_0}\left\{\nabla\cdot\left[\frac{(\nabla\times\boldsymbol{B}_0)_\perp}{B_0}\right]-\frac{\nabla\times\boldsymbol{B}_0\cdot\nabla B_0}{B_0^2}\right\}\ .\end{aligned} \tag{48}$$

For a first glance, Eq. (48) seems to differ from Eq. (46). We calculate the mismatch:

$$\begin{aligned}&\mathrm{PT}_{\mathrm{MHD}}-\mathrm{PT}_{\mathrm{GK}}\\ &= \nabla\cdot\left(\frac{\boldsymbol{b}_0}{B_0}\times\nabla\cdot\delta\mathbb{P}\right)\\ &\quad-\left[\underbrace{\frac{\boldsymbol{b}_0\times\nabla B_0}{B_0^2}\cdot\nabla(\delta P_\perp+\delta P_\parallel)}_{\{1\}}+\underbrace{\frac{\nabla\times\boldsymbol{B}_0}{B_0^2}\cdot\nabla\delta P_\parallel}_{\{2\}}+\underbrace{\frac{\nabla\times\boldsymbol{B}_0\cdot\nabla B_0}{B_0^3}(\delta P_\perp-\delta P_\parallel)}_{\{3\}}\right]\\ &= \frac{\nabla\times\boldsymbol{B}_0}{B_0^2}\cdot\nabla\,\delta P_\perp-\frac{(\nabla\times\boldsymbol{B}_0)_\parallel}{B_0}\cdot\nabla\left(\frac{\delta P_\parallel}{B_0}\right)-\frac{(\nabla\times\boldsymbol{B}_0)_\perp}{B_0}\cdot\nabla\left(\frac{\delta P_\perp}{B_0}\right)\\ &\quad+\frac{\delta P_\parallel}{B_0}\left\{\nabla\cdot\left[\frac{(\nabla\times\boldsymbol{B}_0)_\perp}{B_0}\right]-\frac{\nabla\times\boldsymbol{B}_0\cdot\nabla B_0}{B_0^2}\right\}-\frac{\delta P_\perp}{B_0}\nabla\cdot\frac{(\nabla\times\boldsymbol{B}_0)_\perp}{B_0}\\ &= \underbrace{\frac{(\nabla\times\boldsymbol{B}_0)_\parallel}{B_0^2}\cdot\nabla(\delta P_\perp-\delta P_\parallel)}_{\{4\}}\\ &\quad\underbrace{+2\frac{(\nabla\times\boldsymbol{B}_0)_\perp\cdot\nabla B_0}{B_0^3}(\delta P_\perp-\delta P_\parallel)}_{\{5\}}+\underbrace{\frac{\nabla\cdot[(\nabla\times\boldsymbol{B}_0)_\perp]}{B_0^2}(\delta P_\parallel-\delta P_\perp)}_{\{6\}}\ ,\end{aligned} \tag{49}$$

It can be immediately seen that if $\delta P_\perp = \delta P_\parallel$, the mismatch vanishes. In the case $\delta P_\perp \neq \delta P_\parallel$, assuming $O(\delta P_\perp) \sim O(\delta P_\parallel) \sim O(\delta P_\perp \pm \delta P_\parallel)$, the mismatch is shown to be small compared to the pressure term as follows.

Here we use the scalings of $k_\parallel \ll k_\perp$, $k_\perp R_0 \gg 1$, $O(\beta R_0/L_{P_0}) \sim 1$, and $O((2-s)/q) \sim 1$. We first estimate the order of the terms $\{1\}$, $\{2\}$, $\{3\}$ to find out the leading order of the pressure term.

$$O(\{1\}) \sim \frac{k_\perp}{R_0}\frac{\delta P_{\parallel,\perp}}{B_0} , \tag{50}$$

$$O(\{2\}) \sim \left(\frac{\beta k_\perp}{2L_{P_0}} + \frac{2-s}{q}\frac{k_\parallel}{R_0}\right)\frac{\delta P_{\parallel,\perp}}{B_0} , \tag{51}$$

$$O(\{3\}) \sim \frac{\beta}{2L_{P_0}R_0}\frac{\delta P_{\parallel,\perp}}{B_0} , \tag{52}$$

$$O\left(\frac{\{2\}}{\{1\}}\right) \sim \frac{\beta R_0}{2L_{P_0}} + \frac{2-s}{q}\frac{k_\parallel}{k_\perp} \sim 1 , \tag{53}$$

$$O\left(\frac{\{3\}}{\{1\}}\right) \sim \frac{\beta R_0}{2L_{P_0}}\frac{1}{k_\perp R_0} \ll 1 . \tag{54}$$

The term $\{1\}$ and $\{2\}$ are the leading order terms. Next we only need to compare the mismatch with the term $\{1\}$, which is one of the leading order terms. Using Eqs. (A5) and (A6), we get:

$$O(\{4\}) \sim \frac{2-s}{qB_0R_0}k_\parallel\,\delta P_{\parallel,\perp} , \tag{55}$$

$$O(\{5\}) \sim O(\{6\}) \sim \frac{\beta}{L_{P_0}R_0}\frac{\delta P_{\parallel,\perp}}{B_0} \tag{56}$$

$$O\left(\frac{\{4\}}{\{1\}}\right) \sim \frac{2-s}{q}\frac{k_\parallel}{k_\perp} \ll 1, \tag{57}$$

$$O\left(\frac{\{5\}}{\{1\}}\right) \sim O\left(\frac{\{6\}}{\{1\}}\right) \sim \frac{\beta R_0/L_{P_0}}{k_\perp R_0} \ll 1 . \tag{58}$$

Therefore, the mismatch is not important and the gyrokinetic model reduces to the ideal MHD model with appropriate approximations made.

E. Discussions about the fast ions in different simulation models

There are two major simulation approaches to study the fast ion physics: the pure gyrokinetic approach [3, 4, 10–16] and the hybrid MHD-gyrokinetic approach [17–20]. A typical model for the pure gyrokinetic approach is based on the gyrokinetic equation Eq. (28) and the gyrokinetic field equations, i.e., the gyrokinetic Poisson's equation Eq. (12) and the gyrokinetic Ampère's law Eq. (22). A typical model for the hybrid approach [6] is based on the MHD equations, with the fast ion pressure tensor calculated from the gyrokinetic equation. We have shown that these two models agree with each other in the derivations above, so it makes sense to compare the simulation results from the two different approaches [3, 4].

However, it should be kept in mind that the simulation results should not be expected to be identical even if the geometry, the numerical schemes and other simulation situations are identical, because the agreement between the two models are based on a number of approximations. In the hybrid model, the interaction between the fast ions and the background plasma is reflected only in the pressure term. Although being higher order, the pressure term mismatch between the two models would cause simulation result difference. In the gyrokinetic model, under certain conditions, the fast ions can have other kinds of interactions with the background plasma besides the pressure term. For example, when $k_\perp \rho_f \gtrsim 1$, the expansion of the Bessel function in Eq. (17) is no longer valid. As a result, the terms of order $O(k_\perp^4 \rho_f^4)$ and higher can cause noticeable effects. When the equilibrium flow of either of the ion species is strong enough, i.e., $u_{\parallel 0\alpha} \gtrsim \omega/k_\parallel$ $(\alpha = i, f)$, the FLR term $\{i\}$ in Eq. (35) becomes at least as important as the diamagnetic term $\{ii\}$. When the fast ion distribution is not a (shifted) Maxwellian, Eq. (20) needs to be corrected, causing another difference between the two models. Although most of these effects should be small when the fast ion density is much smaller than the thermal ion density, they may still be noticeable in the simulations.

IV. IMPLEMENTATION OF THE ELECTRON CONTINUITY EQUATION WITH CURRENT

Using the Ampère's law:

$$\frac{c}{4\pi}\boldsymbol{b}_0 \cdot \nabla \times \boldsymbol{B}_0 = \sum_{\alpha \neq e} Z_\alpha n_{0\alpha} u_{\parallel 0\alpha} - e n_{0e} u_{\parallel 0e} \ . \tag{59}$$

Eq. (11) for electron becomes:

$$0 = \partial_t \delta n_e + \delta \boldsymbol{B} \cdot \nabla \left(\sum_{\alpha \neq e} \frac{Z_\alpha n_{0\alpha} u_{\parallel 0\alpha}}{e B_0} - \frac{c}{4\pi e B_0} \boldsymbol{b}_0 \cdot \nabla \times \boldsymbol{B}_0 \right) + \boldsymbol{B}_0 \cdot \nabla \left(\frac{n_{0e}\, \delta u_{\parallel e}}{B_0} \right)$$
$$+ B_0 \boldsymbol{v}_E \cdot \nabla \left(\frac{n_{0e}}{B_0} \right) - n_{0e} (\delta \boldsymbol{v}_{*e} + \boldsymbol{v}_E) \cdot \frac{\nabla B_0}{B_0}$$
$$+ \frac{c \nabla \times \boldsymbol{B}_0}{B_0^2} \cdot \left[\underbrace{- \frac{\nabla\, \delta P_{\parallel e}}{e}}_{\{I\}} \underbrace{- \frac{(\delta P_{\perp e} - \delta P_{\parallel e}) \nabla B_0}{e B_0}}_{\{II\}} + n_{0e} \nabla\, \delta\phi \right] . \tag{60}$$

The term $\{II\}$ comparing to the term $\{I\}$ is of order $1/(k_\perp R_0) \ll 1$, so it can be dropped.

A. Current terms in magnetic coordinates

The magnetic coordinates [1, 21] are used in the GTC, so the equilibrium magnetic field is expressed as:

$$\boldsymbol{B}_0 = g(\psi) \nabla \zeta + I(\psi) \nabla \theta + \delta(\psi, \theta) \nabla \psi \tag{61}$$
$$= q \nabla \psi \times \nabla \theta - \nabla \psi \times \nabla \zeta \ . \tag{62}$$

The Jacobian is:

$$\mathcal{J}^{-1} = \nabla \psi \cdot \nabla \theta \times \nabla \zeta = \frac{B_0^2}{gq + I} \ . \tag{63}$$

The curvature of the magnetic field then writes:

$$\nabla \times \boldsymbol{B}_0 = g' \nabla \psi \times \nabla \zeta + (I' - \partial_\theta \delta) \nabla \psi \times \nabla \theta \ , \tag{64}$$

where the prime symbol ($'$) denotes the derivative with respect to ψ. The parallel component writes:

$$\boldsymbol{b}_0 \cdot \nabla \times \boldsymbol{B}_0 = B_0 \frac{g(I' - \partial_\theta \delta) - I g'}{gq + I} \ . \tag{65}$$

The second term in Eq. (60) can be expanded into two components:

$$\frac{Z_\alpha}{e} \delta \boldsymbol{B} \cdot \nabla \left(\frac{n_{0\alpha} u_{\parallel 0\alpha}}{B_0} \right)$$
$$\approx \frac{Z_\alpha}{e} \nabla\, \delta A_\parallel \times \boldsymbol{b}_0 \cdot \nabla \left(\frac{n_{0\alpha} u_{\parallel 0\alpha}}{B_0} \right)$$
$$= \frac{\mathcal{J}^{-1}}{B_0} \left[(g \partial_\theta\, \delta A_\parallel - I \partial_\zeta\, \delta A_\parallel) \partial_\psi \left(\frac{n_{0\alpha} u_{\parallel 0\alpha}}{B_0} \right) + (\delta \partial_\zeta\, \delta A_\parallel - g \partial_\psi\, \delta A_\parallel) \partial_\theta \left(\frac{n_{0\alpha} u_{\parallel 0\alpha}}{B_0} \right) \right.$$
$$\left. + (I \partial_\psi\, \delta A_\parallel - \delta \partial_\theta\, \delta A_\parallel) \partial_\zeta \left(\frac{n_{0\alpha} u_{\parallel 0\alpha}}{B_0} \right) \right] . \tag{66}$$

$$
\begin{aligned}
&-\frac{c}{4\pi e}\delta\boldsymbol{B}\cdot\nabla\left(\frac{\boldsymbol{b}_0\cdot\nabla\times\boldsymbol{B}_0}{B_0}\right)\\
&\approx -\frac{c}{4\pi e}\nabla\,\delta A_\parallel\times\boldsymbol{b}_0\cdot\nabla\left[\frac{g(I'-\partial_\theta\delta)-Ig'}{gq+I}\right]\\
&=\frac{c}{4\pi e}\frac{\mathcal{J}^{-1}}{B_0}\left[-g(\partial_\psi S)(\partial_\theta\,\delta A_\parallel)+\left(I\partial_\psi S+\frac{g\delta\partial_\theta^2\delta}{gq+I}\right)(\partial_\zeta\,\delta A_\parallel)-\frac{g^2\partial_\theta^2\delta}{gq+I}(\partial_\psi\,\delta A_\parallel)\right]\ ,
\end{aligned}
\tag{67}
$$

where

$$
\begin{aligned}
\partial_\psi S&=\partial_\psi\left[\frac{g(I'-\partial_\theta\delta)-Ig'}{gq+I}\right]\\
&=\frac{g(I''-\partial_\psi\partial_\theta\delta)-g'\partial_\theta\delta-Ig''}{gq+I}-\frac{[g(I'-\partial_\theta\delta)-Ig'](g'q+gq'+I')}{(gq+I)^2}\ .
\end{aligned}
\tag{68}
$$

The last term in Eq. (60) becomes the summation of these two terms:

$$
-\frac{c\nabla\times\boldsymbol{B}_0}{eB_0^2}\cdot\nabla\,\delta P_{e\parallel}=-\frac{c}{e(gq+I)}[-g'\partial_\theta\,\delta P_{e\parallel}+(I'-\partial_\theta\delta)\partial_\zeta\,\delta P_{e\parallel}]\ .\tag{69}
$$

$$
n_{e0}\frac{c\nabla\times\boldsymbol{B}_0}{B_0^2}\cdot\nabla\,\delta\phi=\frac{n_{e0}c}{gq+I}[-g'\partial_\theta\,\delta\phi+(I'-\partial_\theta\delta)\partial_\zeta\,\delta\phi]\ .\tag{70}
$$

B. Normalization of the current terms

Follow the normalization units and symbols in Ref. [1]. Normalize Eq. (60) to be:

$$
\begin{aligned}
0=\partial_t\,\delta n_e&+\sum_{\alpha\neq e}Z_\alpha\,\delta\boldsymbol{B}\cdot\nabla\left(\frac{n_{0\alpha}u_{\parallel0\alpha}}{B_0}\right)-\frac{2}{\beta_a}\frac{\rho_a^2}{R_0^2}\delta\boldsymbol{B}\cdot\nabla\left(\frac{\boldsymbol{b}_0\cdot\nabla\times\boldsymbol{B}_0}{B_0}\right)\\
&+\boldsymbol{B}_0\cdot\nabla\left(\frac{n_{e0}\,\delta u_{e\parallel}}{B_0}\right)+B_0\boldsymbol{v}_E\cdot\nabla\left(\frac{n_{e0}}{B_0}\right)-n_{e0}(\boldsymbol{v}_{e*}+\boldsymbol{v}_E)\cdot\frac{\nabla B_0}{B_0}\\
&+\frac{\nabla\times\boldsymbol{B}_0}{B_0^2}\cdot\left[-\nabla\,\delta P_{e\parallel}-\frac{(\delta P_{\perp e}-\delta P_{\parallel e})\nabla B_0}{B_0}+n_{e0}\cdot\nabla\,\delta\phi\right]\ ,
\end{aligned}
\tag{71}
$$

where

$$
\beta_a=\frac{8\pi n_a T_a}{B_a^2}\ ,\tag{72}
$$

$$
\rho_a^2=\frac{T_a}{m_p\Omega_p^2}\ ,\tag{73}
$$

with T_a being the electron on-axis temperature. Normalizing Eqs. (66)–(70):

$$
\begin{aligned}
&Z_\alpha\delta\boldsymbol{B}\cdot\nabla\left(\frac{n_{0\alpha}u_{\parallel0\alpha}}{B_0}\right)\\
&=\frac{\mathcal{J}^{-1}}{B_0}\left[(g\partial_\theta\,\delta A_\parallel-I\partial_\zeta\,\delta A_\parallel)\partial_\psi\left(\frac{n_{0\alpha}u_{\parallel0\alpha}}{B_0}\right)+(\delta\partial_\zeta\,\delta A_\parallel-g\partial_\psi\,\delta A_\parallel)\partial_\theta\left(\frac{n_{0\alpha}u_{\parallel0\alpha}}{B_0}\right)\right.\\
&\left.+(I\partial_\psi\,\delta A_\parallel-\delta\partial_\theta\,\delta A_\parallel)\partial_\zeta\left(\frac{n_{0\alpha}u_{\parallel0\alpha}}{B_0}\right)\right]\ ,
\end{aligned}
\tag{74}
$$

$$-\frac{2}{\beta_a}\frac{\rho_a^2}{R_0^2}\delta\boldsymbol{B}\cdot\nabla\left(\frac{\boldsymbol{b}_0\cdot\nabla\times\boldsymbol{B}_0}{B_0}\right)$$
$$=\frac{2}{\beta_a}\frac{\rho_a^2}{R_0^2}\frac{\mathcal{J}^{-1}}{B_0}\left[-g(\partial_\psi S)(\partial_\theta\,\delta A_\parallel)+\left(I\partial_\psi S+\frac{g\delta\partial_\theta^2\delta}{gq+I}\right)(\partial_\zeta\,\delta A_\parallel)-\frac{g^2\partial_\theta^2\delta}{gq+I}(\partial_\psi\,\delta A_\parallel)\right] ,\tag{75}$$

$$\partial_\psi S=\partial_\psi\left[\frac{g(I'-\partial_\theta\delta)-Ig'}{gq+I}\right]$$
$$=\frac{g(I''-\partial_\psi\partial_\theta\delta)-g'\partial_\theta\delta-Ig''}{gq+I}-\frac{[g(I'-\partial_\theta\delta)-Ig'](g'q+gq'+I')}{(gq+I)^2} ,\tag{76}$$

$$-\frac{\nabla\times\boldsymbol{B}_0}{B_0^2}\cdot\nabla\,\delta P_{e\parallel}=-\frac{1}{gq+I}[-g'\partial_\theta\,\delta P_{e\parallel}+(I'-\partial_\theta\delta)\partial_\zeta\,\delta P_{e\parallel}] ,\tag{77}$$

$$n_{e0}\frac{\nabla\times\boldsymbol{B}_0}{B_0^2}\cdot\nabla\,\delta\phi=\frac{n_{e0}}{gq+I}[-g'\partial_\theta\,\delta\phi+(I'-\partial_\theta\delta)\partial_\zeta\,\delta\phi] .\tag{78}$$

V. EXTEND THE MAGNETIC FIELD MODEL TO RECOVER FINITE $\nabla\times\boldsymbol{B}_0$

In this section we keep using the normalized quantities. All quantities in this section are equilibrium quantities, so the equilibrium subscript 0 for the magnetic field is omitted. Previously in the GTC, an s-α like (cyclone) magnetic field model (citation?) is used:

$$B=1-\epsilon\cos\theta+O(\epsilon^2) ,\tag{79}$$
$$I=0+O(\epsilon^2) ,\tag{80}$$
$$g=1+O(\epsilon^2) ,\tag{81}$$
$$\delta=0+O(\epsilon) ,\tag{82}$$
$$\theta=\theta_0+O(\epsilon) ,\tag{83}$$
$$\zeta=\zeta_0+O(\epsilon) ,\tag{84}$$

where $\epsilon=r/R_0$ is the normalized radial coordinate, θ_0 and ζ_0 are the geometric poloidal and toroidal angles, and θ and ζ are the corresponding magnetic coordinates. Such a field model makes all the derivatives of g and I zero, and thus leading to zero equilibrium current terms. Here we extend this field model to a higher-order one to recover the equilibrium current.

Assume concentric circular magnetic surfaces.

$$'=\frac{\mathrm{d}}{\mathrm{d}\psi}=\frac{\mathrm{d}\epsilon}{\mathrm{d}\psi}\frac{\mathrm{d}}{\mathrm{d}\epsilon}=\frac{q}{\epsilon}\frac{\mathrm{d}}{\mathrm{d}\epsilon} ,\tag{85}$$

In the large-aspect-ratio limit, we expand the field related quantities with respect to ϵ:

$$B = 1 - \epsilon \cos\theta_0 + \epsilon^2 B_2 + \epsilon^3 B_3 + \cdots \ , \tag{86}$$

$$I = \epsilon^2 I_2 + \epsilon^3 I_3 + \cdots \ , \tag{87}$$

$$g = 1 + \epsilon^2 g_2 + \epsilon^3 g_3 + \cdots \ , \tag{88}$$

$$\theta = \theta_0 + \epsilon\theta_1 + \epsilon^2\theta_2 + \cdots \ , \tag{89}$$

$$\zeta = \zeta_0 + \epsilon\zeta_1 + \epsilon^2\zeta_2 + \cdots \ , \tag{90}$$

where g_i and I_i $(i = 2, 3, \cdots)$ are functions of the safety factor q; and B_i, θ_i, and ζ_i $(i = 1, 2, \cdots)$ are periodic functions of θ_0.

We want the field model to satisfy these conditions:

- The Jacobian satisfies $\mathcal{J}^{-1} = \nabla\psi \cdot \nabla\theta \times \nabla\zeta = B^2/(gq + I)$ so that I is a function of only ψ (equivalently ϵ, because of concentric circular flux surfaces).

- The radial component of the field is zero because of concentric circular flux surfaces: $B_\epsilon = \epsilon\delta/q + I\partial_\epsilon\theta + g\partial_\epsilon\zeta = 0$.

- The field magnitude expression is consistent with the covariant representation: $B = |\delta\nabla\psi + I\nabla\theta + g\nabla\zeta|$.

- The field line is straight in the (θ, ζ) space, so $\boldsymbol{B} \cdot \nabla\zeta/(\boldsymbol{B} \cdot \nabla\theta) = q(\psi)$ with q being the safety factor which is independent of θ and ζ.

Plug the expansions Eqs. (86)–(90) into the above conditions, and solving them up to the

$O(\epsilon)$ order gives:

$$B = 1 - \epsilon \cos\theta_0 + O(\epsilon^2) \ , \tag{91}$$

$$\delta = \epsilon \sin\theta_0 + O(\epsilon^2) = \epsilon \sin\theta + O(\epsilon^2) \ , \tag{92}$$

$$I = \frac{\epsilon^2}{q} + O(\epsilon^4) \ , \tag{93}$$

$$I' = 2 - s + O(\epsilon^2) \ , \tag{94}$$

$$g = 1 + O(\epsilon^2) \ , \tag{95}$$

$$g' = O(\epsilon^0) \ , \tag{96}$$

$$\theta = \theta_0 - \epsilon \sin\theta_0 + O(\epsilon^2) \ , \tag{97}$$

$$\theta_0 = \theta + \epsilon \sin\theta + O(\epsilon^2) \ , \tag{98}$$

$$\zeta = \zeta_0 + O(\epsilon^4) \ , \tag{99}$$

$$\nabla \times \boldsymbol{B}_0 = O(\epsilon^0)\nabla\psi \times \nabla\zeta + [(2-s) - \epsilon\cos\theta + O(\epsilon^2)]\nabla\psi \times \nabla\theta \ , \tag{100}$$

$$\boldsymbol{b}_0 \cdot \nabla \times \boldsymbol{B}_0 = \frac{\mathcal{J}^{-1}}{B_0}[(2-s) - \epsilon\cos\theta_0 + O(\epsilon)] \ . \tag{101}$$

Although it is straightforward to solve the equations up to the $O(\epsilon^2)$ order, such a model would not be very useful because other effects come into play at the order of $O(\epsilon^2)$ or even lower, such as the Shafranov shift, and the finite pressure gradient effect. The field model of order $O(\epsilon)$, i.e., Eqs. (91)–(99), is good enough to recover the parallel current and is therefore implemented. It is straightforward to show that in Eqs. (74)–(78) the terms containing the nonorthogonality factor δ are one order smaller than the leading order and thus are dropped in the implementation for simplicity.

VI. EQUILIBRIUM CURRENT EFFECT ON THE RSAE

A. Analytic calculation

In a simple geometry with concentric-circular flux surfaces, in the uniform plasma and zero-β limit, considering only one n and m harmonic $\delta\phi(r,\theta,\zeta) = \delta\hat{\phi}(r)\exp[i(n\zeta - m\theta)]$, Eq. (42) near the $q_{\min}$ surface becomes [3]:

$$\frac{1}{r}\frac{\mathrm{d}}{\mathrm{d}r}\left(r\Lambda\frac{\mathrm{d}}{\mathrm{d}r}\delta\hat{\phi}\right) - \frac{m^2}{r^2}\Lambda\,\delta\hat{\phi} - \frac{D}{r}\delta\hat{\phi} = 0 \ , \tag{102}$$

where

$$\Lambda = \frac{\omega^2}{v_A^2} - k_\parallel^2 \ , \tag{103}$$

D represents contributions from fast ion pressure, background plasma pressure gradient, toroidal coupling, magnetic shear, etc. The first two terms of Eq. (102) give the Alfvén continuum. The last term determines whether an eigenmode exists near the Alfvén continuum extremum. Here we only consider the magnetic shear effect. When the equilibrium current is ignored,

$$D = k_{\|} k'_{\|} + r k_{\|} k''_{\|} \ . \tag{104}$$

At the $q_{\min}$ surface, noting that $k'_{\|} = 0$ and $k''_{\|} \neq 0$, D is non-zero and an RSAE exists as can be shown by numerically solving Eq. (102). With the equilibrium current recovered,

$$D = -2 k_{\|} k'_{\|} \ , \tag{105}$$

which is zero at the $q_{\min}$ surface and thus eigenmode does not exist. Note that other effects contributing to D mentioned above may bring back the eigenmode.

B. Verification in simulation

To verify the implementation of the current, we simulate a case in a simple geometry which should recover what the analytic calculation shows. The parameters are taken from Ref. [3]. The q-profile is shown in Fig. 1(a), whose corresponding Alfvén continua of $n = 4, m = 6$ and $n = 4, m = 7$ without coupling are shown in Fig. 1(b). The $n = 4, m = 6$ mode is studied here to avoid distraction by the toroidal coupling effect, because the toroidal coupling effect cannot make an RSAE below the continuum minimum [22]. In the ideal MHD limit, the RSAE exists when the equilibrium current is not taken into account.

The differences between the simulations without and with equilibrium current can mainly be seen in the contour plots of $\delta\phi$ in the radial-time space in Fig. 2. In Fig. 2(a), which is corresponding to the case without equilibrium current, as an eigenmode exists, the mode structures are horizontal, indicating that $\delta\phi$ at every radial location oscillates at the same eigenmode frequency. For the case with equilibrium current shown in Fig. 2(b), since no eigenmode exists, $\delta\phi$ at every radial location oscillates at the local continuum frequency, leading to the bending of the mode structures or the so-called phase-mixing. The quick damping of the mode amplitude in Fig. 2(b) also indicates that there is no eigenmode in this case. Therefore, the simulation results are consistent with the analytic calculation in Sec. VI A

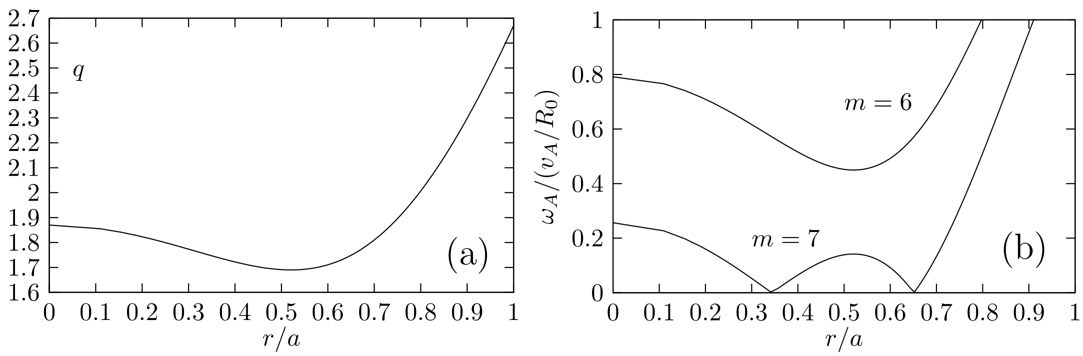

FIG. 1. (a) Safety factor q-profile. (b) Alfvén continua of $n = 4, m = 6$ and $n = 4, m = 7$ in ideal MHD limit and without linear coupling.

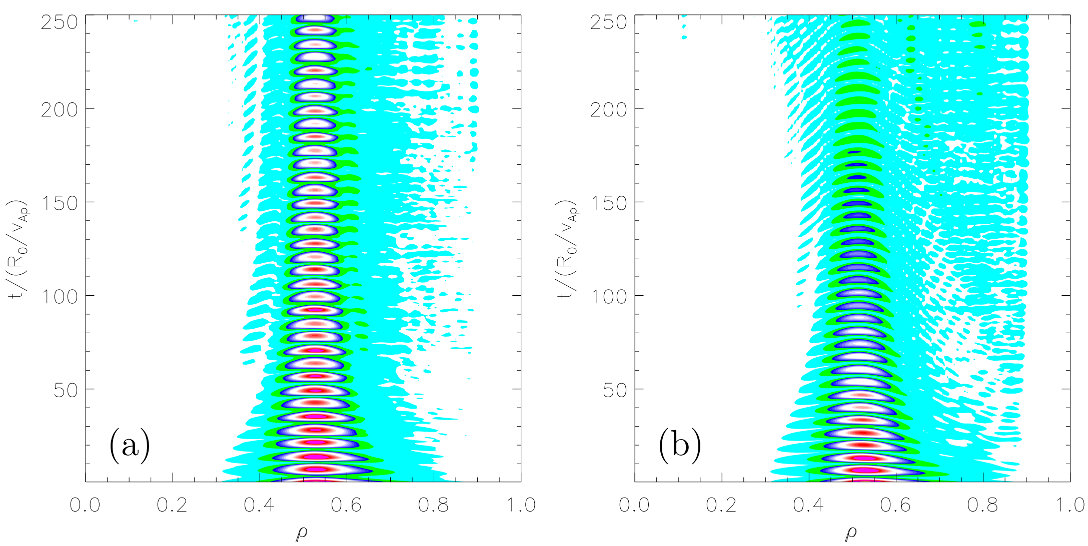

FIG. 2. Contour plots of $\delta\phi$ in the radial-time space in RSAE simulations (a) without equilibrium current; (b) with equilibrium current. The time is normalized to R_0/v_{Ap}, where v_{Ap} is defined as $v_{Ap} = B_a/\sqrt{4\pi n_a m_p}$

VII. SIMULATIONS OF DIII-D DISCHARGE #142111 AT 750ms

One of the most significant energetic-particle-driven modes in the DIII-D discharge #142111 at the time of 750ms is the RSAE. The magnetic field, including the flux surface structure, field magnitude, and the q-profile, the density and the temperature profiles of all three species, i.e., the electron, the background ion, and the fast ion, are loaded from the experimental data into the GTC. The equilibrium profiles are shown in Fig. 3. The $q_{\min}$ surfaces is at $\rho = 0.33$ where ρ is the square root of the normalized toroidal flux. $q_{\min}$ takes

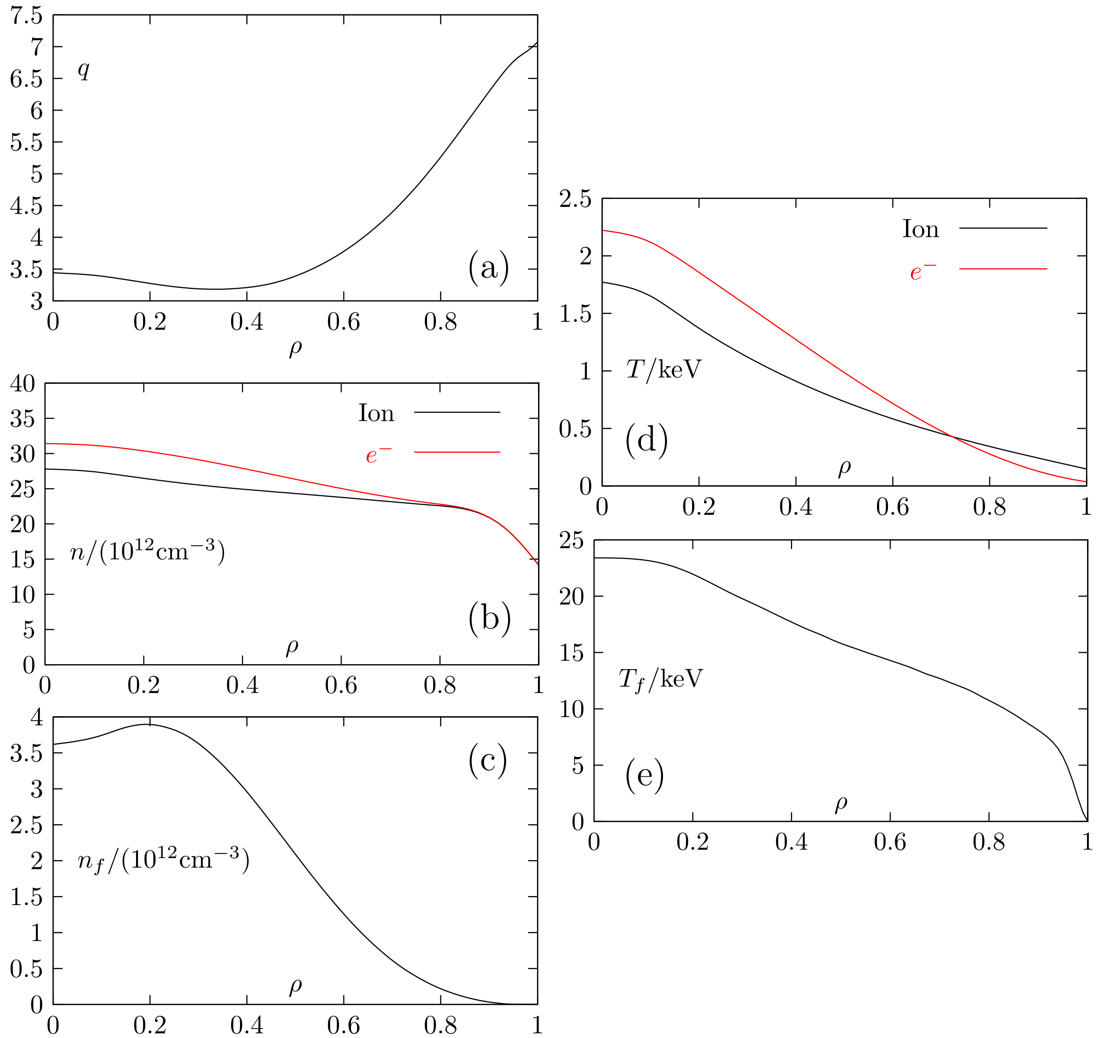

FIG. 3. Equilibrium profiles in DIII-D discharge #142111 at 750ms: (a) q-profile, (b) background plasma density, (c) fast ion density, (d) background plasma temperature, (f) fast ion temperature.

the value 3.1828. Both ion species are deuterium nuclei.

The $n = 3$ and $n = 4$ modes have been successfully simulated, respectively. For the $n = 3$ mode, before adding in the fast ions, the background plasma pressure effects are tested. When fast ions are not loaded, the thermal ion density is loaded to be the same as the electron density so as to retain neutrality. In the zero temperature ideal MHD limit, giving an initial perturbation near the $q_{\min}$ surface produces an RSAE-like mode shown in Fig. 4(a) and (b). The mode frequency is listed as the case (I) in Table I and marked on the Alfvén continuum plot in Fig. 5(a). To study the finite-β effect, various simulation cases are done as listed in Table I and their frequencies are marked on the corresponding Alfvén

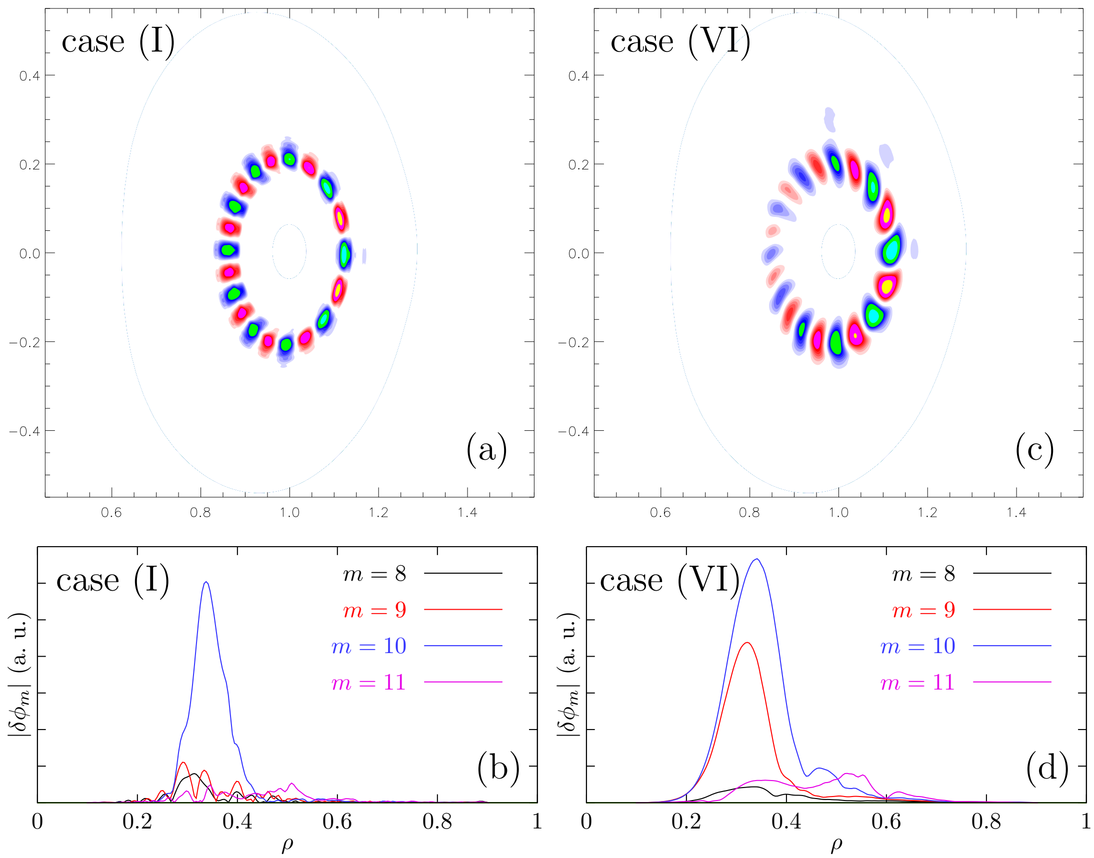

FIG. 4. Mode structures for $n = 3$ mode: (a)(c) poloidal contour plots of $\delta\phi$ for case (I) and case (VI), respectively, (b)(d) m-harmonic decomposed $\delta\phi$ for case (I) and case (VI), respectively.

continuum plots in Fig. 5. The Alfvén continua are calculated using the m-spectral method in the slow sound approximation described in Appendix B with the kinetic consideration [23]: $\gamma_s P_0 = P_{0e} + 7P_{0i}/4$. Adding in the finite electron temperature from case (I) to case (II) raises the Alfvén continua and the mode frequency due to the electron geodesic compressibility. From case (II) to case (III) the ion geodesic compressibility is recovered to raise the continua and mode frequencies even more. In case (III) due to the presence of the ion pressure gradient, the ion kinetic damping cannot be seen, so in case (IV) the pressure gradient drive is artificially suppressed to show the damping effect. Moving the ion pressure effect to be carried by electrons and getting the same mode frequency, case (V) shows that other than the 7/4 coefficient for ion, the ion pressure and the electron pressure contribute to the mode frequency in a very similar way.

When the fast ions are added, which is the case (VI) in Table I, the mode frequency is

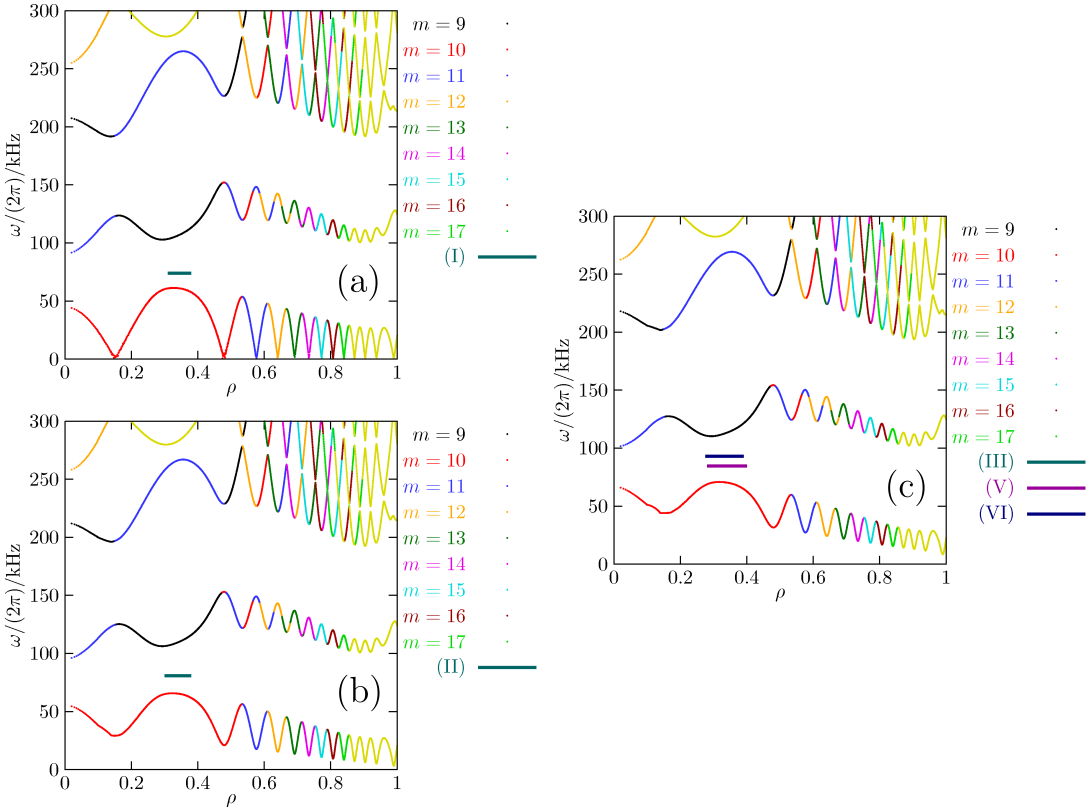

FIG. 5. Alfvén continua with slow sound approximation for $n = 3$: (a) zero-β limit, (b) only include electron β, (c) complete background plasma β. The horizontal lines are the frequencies obtained in various simulation cases described in Table I. The width of each horizontal line represents the FWHM of the mode structure.

further raised. The non-perturbative mode structure modification by fast ions can be seen in the poloidal mode structure in Fig. 4(c). In the m-harmonic decomposition plot in Fig. 4(d), it can be seen that besides the dominant $m = 10$ harmonic, there is a sub-dominant $m = 9$ harmonic. This is because the time 750ms is during the mode transition from RSAE to TAE [22]. The mode seen in simulation is something between an RSAE and a TAE. In one situation it may be more RSAE-like, such as the cases (I)-(V). In another situation it could be more TAE-like, such as the fast ion driven case (VI).

($n = 4$ case pending to add)

TABLE I. Various simulation cases and resulted frequencies to test the finite-β effect on the $n = 3$ mode

Case	Description	$(\omega_r, \gamma)/(v_{Ap}/R_0)$	$(\omega_r, \gamma)/(2\pi)/\mathrm{kHz}$	γ/ω_r
(I)	Zero temperature ideal MHD	0.103	73.8	
(II)	Finite $\delta E_\parallel$, adiabatic e^- with real T_e profile and kinetic ions with only 2% of real T_i	$(0.113, -0.00208)$	$(80.9, -1.49)$	-0.0185
(III)	Same as case (II) except for real T_i profile recovered	0.118	84.7	
(IV)	Same as case (III) except that kinetic ion gradient drive is artificially suppressed	(pending measure)		
(V)	Same as case (II) except that electrons carry the total pressure ($T_e \leftarrow T_e + 7T_i/4$)	$(0.118, -0.00273)$	$(84.6, -1.96)$	-0.0231
(VI)	Same as case (IV) except that fast ions are added in	$(0.130, 0.00919)$	$(92.9, 6.59)$	0.0710

Appendix A: Estimation of some magnetic field parameters in a tokamak

Noticing the safety factor $q \approx rB_\zeta/(R_0 B_\theta) = \epsilon B_\zeta/B_\theta$, the equilibrium magnetic field writes:

$$\begin{aligned} \boldsymbol{B}_0 &= B_\theta \hat{\boldsymbol{\theta}} + B_\zeta \hat{\boldsymbol{\zeta}} \\ &= B_\zeta \left(\frac{\epsilon}{q} \hat{\boldsymbol{\theta}} + \hat{\boldsymbol{\zeta}} \right) \ . \end{aligned}$$

where B_θ and B_ζ are the poloidal and the toroidal component, respectively, while $\hat{\boldsymbol{\theta}}$ and $\hat{\boldsymbol{\zeta}}$ are the unit vectors in the poloidal and the toroidal direction, respectively. The toroidal vacuum field writes:

$$B_\zeta = \frac{B_a R_0}{R} = \frac{B_a}{1 + \epsilon \cos\theta} \ . \tag{A1}$$

This can be used to estimate the parallel component of $\nabla \times \boldsymbol{B}_0$:

$$\begin{aligned} (\nabla \times \boldsymbol{B}_0)_\parallel &\approx \frac{\hat{\boldsymbol{\zeta}}}{r} \left[\partial_r \left(r \frac{\epsilon}{q} B_\zeta \right) \right] \\ &\approx \hat{\boldsymbol{\zeta}} \frac{B_0}{qR_0} (2 - s) \ , \end{aligned} \tag{A2}$$

where

$$s = \frac{r}{q} \frac{\mathrm{d}q}{\mathrm{d}r} \tag{A3}$$

is the magnetic shear. For the perpendicular component of $\nabla \times \boldsymbol{B}_0$, the force balance equation is used:

$$\begin{aligned} \nabla P_0 &= \frac{1}{c}\boldsymbol{J}_0 \times \boldsymbol{B}_0 \\ &= \frac{1}{4\pi}(\nabla \times \boldsymbol{B}_0) \times \boldsymbol{B}_0 \ . \end{aligned} \tag{A4}$$

Take $\boldsymbol{b}_0\times$ Eq. (A4) to get:

$$(\nabla \times \boldsymbol{B}_0)_\perp = \frac{4\pi}{B_0}\boldsymbol{b}_0 \times \nabla P_0 \ . \tag{A5}$$

Meanwhile,

$$\begin{aligned} &\nabla \cdot [(\nabla \times \boldsymbol{B}_0)_\perp] \\ &= 4\pi \nabla \cdot \left(\frac{\boldsymbol{b}_0}{B_0} \times \nabla P_0\right) \\ &= \frac{4\pi}{B_0^2}(\nabla \times \boldsymbol{B}_0 + 2\boldsymbol{b}_0 \times \nabla B_0) \cdot \nabla P_0 \ . \end{aligned} \tag{A6}$$

We also have:

$$\nabla B_0 \approx -\frac{B_a R_0}{R^2}\hat{\boldsymbol{R}} \approx -\frac{B_0}{R_0}(\hat{\boldsymbol{r}}\cos\theta - \hat{\boldsymbol{\theta}}\sin\theta) \tag{A7}$$

$$\boldsymbol{b}_0 \times \nabla B_0 \approx \frac{B_0}{R_0}\left[-\hat{\boldsymbol{r}}\sin\theta - \hat{\boldsymbol{\theta}}\cos\theta + \hat{\boldsymbol{\zeta}}\frac{\epsilon}{q}\cos\theta\right] \tag{A8}$$

Appendix B: Alfvén continuum calculation

In realistic situations, simple estimation of the Alfvén continuum like $\omega_A \approx (nq - m)v_A/(qR_0)$ is not good enough. Such an estimation would introduce fairly large inaccuracy by geometric effects, finite-β effect, etc. In this section an m-spectral method is used to solve the ideal MHD Alfvén continuum equation [24] in the slow sound (low-β) approximation [25].

The Alfvén continuum equation writes [24]:

$$\begin{pmatrix} \mathbb{E}_{11} & \mathbb{E}_{12} \\ \mathbb{E}_{21} & \mathbb{E}_{22} \end{pmatrix} \begin{pmatrix} \xi_s \\ \nabla \cdot \boldsymbol{\xi} \end{pmatrix} = 0 \ , \tag{B1}$$

where

$$\mathbb{E}_{11} = \frac{4\pi\rho_M\omega^2|\nabla\psi|^2}{B_0^2} + \boldsymbol{B}_0\cdot\nabla\left(\frac{|\nabla\psi|^2\boldsymbol{B}_0\cdot\nabla}{B_0^2}\right) \ , \tag{B2}$$

$$\mathbb{E}_{12} = 4\pi\gamma_s P_0\kappa_s \ , \tag{B3}$$

$$\mathbb{E}_{21} = \kappa_s \ , \tag{B4}$$

$$\mathbb{E}_{22} = \frac{4\pi\gamma_s P_0 + B_0^2}{B_0^2} + \frac{\gamma_s P_0}{\rho_M\omega^2}\boldsymbol{B}_0\cdot\nabla\left(\frac{\boldsymbol{B}_0\cdot\nabla}{B_0^2}\right) \ . \tag{B5}$$

$$\kappa_s = 2\boldsymbol{\kappa}\cdot\frac{\boldsymbol{B}_0\times\nabla\psi}{B_0^2} \ , \tag{B6}$$

$$\boldsymbol{\kappa} = \boldsymbol{b}_0\cdot\nabla\boldsymbol{b}_0 = (\nabla\times\boldsymbol{b}_0)\times\boldsymbol{b}_0 \ . \tag{B7}$$

Using the magnetic coordinates mentioned in Sec. IV A, some vector expressions can be simplified:

$$\boldsymbol{B}_0\cdot\nabla = \mathcal{J}^{-1}(\partial_\theta + q\partial_\zeta) \ , \tag{B8}$$

$$\kappa_s = -\frac{2\mathcal{J}^{-1}}{B_0}g\left(\partial_\theta\frac{1}{B_0}\right) = \frac{2\mathcal{J}^{-1}g}{B_0^3}\partial_\theta B_0 \ . \tag{B9}$$

In the GTC, $|\nabla\psi|^2$ can be calculated using the splines of the poloidal Cartesian coordinates (X, Z):

$$|\nabla\psi|^2 = (\partial_X\psi)^2 + (\partial_Z\psi)^2 = \left(\frac{1}{\partial_\psi X - \partial_\theta X\frac{\partial_\psi Z}{\partial_\theta Z}}\right)^2 + \left(\frac{1}{\partial_\psi Z - \partial_\theta Z\frac{\partial_\psi X}{\partial_\theta X}}\right)^2 \ . \tag{B10}$$

Equation (B1) is an eigenvalue equation with ω^2 being the eigenvalue. The second term of $\mathbb{E}_{22}$ is ω-dependent, which complicates the problem. However, comparing to the first term gives:

$$\frac{\frac{\gamma_s P_0}{\rho_M\omega^2}\boldsymbol{B}_0\cdot\nabla\left(\frac{\boldsymbol{B}_0\cdot\nabla}{B_0^2}\right)}{\frac{4\pi\gamma_s P_0 + B_0^2}{B_0^2}} = \frac{-4\pi\gamma_s P_0 k_\parallel^2/(4\pi\rho_M\omega^2)}{(4\pi\gamma_s P_0 + B_0^2)/B_0^2} \approx \frac{-4\pi\gamma_s P_0/B_0^2}{(4\pi\gamma_s P_0 + B_0^2)/B_0^2} \sim O\left(\frac{\beta}{\beta+1}\right) \ , \tag{B11}$$

This shows the second term of $\mathbb{E}_{22}$ can be dropped in the low-β limit, which is the slow sound approximation in Ref. [25]. In this approximation, Eq. (B1) becomes:

$$\left[4\pi\rho_M\omega^2\frac{|\nabla\psi|^2}{\mathcal{J}^{-1}B_0^2} + \frac{\boldsymbol{B}_0\cdot\nabla}{\mathcal{J}^{-1}}\left(\frac{|\nabla\psi|^2\boldsymbol{B}_0\cdot\nabla}{B_0^2}\right) - \frac{4\pi\gamma_s P_0\kappa_s^2 B_0^2}{\mathcal{J}^{-1}(4\pi\gamma_s P_0 + B_0^2)}\right]\xi_s = 0 \ . \tag{B12}$$

Expanding θ-dependent quantities as summations of m-harmonics:

$$\xi_s = e^{in\zeta}\sum_m (\xi_s)_m e^{-im\theta} \ , \tag{B13}$$

$$\begin{pmatrix} \frac{|\nabla\psi|^2\mathcal{J}^{-1}}{B_0^2} \\ \frac{|\nabla\psi|^2}{B_0^2\mathcal{J}^{-1}} \\ \frac{4\pi\gamma_s P_0\kappa_s^2 B_0^2}{\mathcal{J}^{-1}(4\pi\gamma_s P_0+B_0^2)} \end{pmatrix} = \sum_m \begin{pmatrix} \left(\frac{|\nabla\psi|^2\mathcal{J}^{-1}}{B_0^2}\right)_m \\ \left(\frac{|\nabla\psi|^2}{B_0^2\mathcal{J}^{-1}}\right)_m \\ \left(\frac{4\pi\gamma_s P_0\kappa_s^2 B_0^2}{\mathcal{J}^{-1}(4\pi\gamma_s P_0+B_0^2)}\right)_m \end{pmatrix} e^{im\theta} \ . \tag{B14}$$

Using $\{e^{-im\theta}\}$ as basis, Eq. (B12) can be written in this matrix form:

$$(\mathbb{G}^\dagger\mathbb{H}\mathbb{G} + \mathbb{N})\xi_s = 4\pi\rho_M\omega^2\mathbb{J}\xi_s \ , \tag{B15}$$

which is a generalized eigenvalue problem, with $4\pi\rho_M\omega^2$ being the eigenvalue,

$$\xi_s = (\cdots, (\xi_s)_{m-1}, (\xi_s)_m, (\xi_s)_{m+1}, \cdots)^T \tag{B16}$$

being the eigenvector. The operator matrices and their elements are:

$$\mathbb{G} = -i\frac{\boldsymbol{B}_0\cdot\nabla}{\mathcal{J}^{-1}} \qquad \mathbb{G}_{m,m'} = (nq-m)\delta_{m,m'} \tag{B17}$$

$$\mathbb{H} = \frac{|\nabla\psi|^2\mathcal{J}^{-1}}{B_0^2} \qquad \mathbb{H}_{m,m'} = \left(\frac{|\nabla\psi|^2\mathcal{J}^{-1}}{B_0^2}\right)_{m'-m} \tag{B18}$$

$$\mathbb{J} = \frac{|\nabla\psi|^2}{B_0^2\mathcal{J}^{-1}} \qquad \mathbb{J}_{m,m'} = \left(\frac{|\nabla\psi|^2}{B_0^2\mathcal{J}^{-1}}\right)_{m'-m} \tag{B19}$$

$$\mathbb{N} = \frac{4\pi\gamma_s P_0\kappa_s^2 B_0^2}{\mathcal{J}^{-1}(4\pi\gamma_s P_0 + B_0^2)} \qquad \mathbb{N}_{m,m'} = \left(\frac{4\pi\gamma_s P_0\kappa_s^2 B_0^2}{\mathcal{J}^{-1}(4\pi\gamma_s P_0 + B_0^2)}\right)_{m'-m} \tag{B20}$$

A code based on the eigenvalue library SLEPc [26] is written to solve Eq. (B15) to give the Alfvén continuum plots in Sec. VII.

[1] I. Holod, W. L. Zhang, Y. Xiao, and Z. Lin, Physics of Plasmas **16**, 122307 (2009).

[2] Z. Lin, T. S. Hahm, W. W. Lee, W. M. Tang, and R. B. White, Science **281**, 1835 (1998).

[3] W. Deng, Z. Lin, I. Holod, X. Wang, Y. Xiao, and W. Zhang, Physics of Plasmas **17**, 112504 (2010).

[4] H. S. Zhang, Z. Lin, I. Holod, X. Wang, Y. Xiao, and W. L. Zhang, Physics of Plasmas **17**, 112505 (2010).

[5] M. N. Bussac, R. Pellat, D. Edery, and J. L. Soule, Phys. Rev. Lett. **35**, 1638 (1975).

[6] W. Park, S. Parker, H. Biglari, M. Chance, L. Chen, C. Z. Cheng, T. S. Hahm, W. W. Lee, R. Kulsrud, D. Monticello, L. Sugiyama, and R. White, Physics of Fluids B: Plasma Physics **4**, 2033 (1992).

[7] W. Lee, Journal of Computational Physics **72**, 243 (1987).

[8] Z. Lin and W. W. Lee, Phys. Rev. E **52**, 5646 (1995).

[9] H. Biglari and L. Chen, Phys. Rev. Lett. **67**, 3681 (1991).

[10] P. Lauber, S. Gunter, and S. D. Pinches, Physics of Plasmas **12**, 122501 (2005).

[11] Y. Nishimura, Z. Lin, and W. X. Wang, Physics of Plasmas **14**, 042503 (2007).

[12] W. Zhang, Z. Lin, and L. Chen, Phys. Rev. Lett. **101**, 095001 (2008).

[13] Y. Nishimura, Physics of Plasmas **16**, 030702 (2009).

[14] A. Mishchenko, A. Konies, and R. Hatzky, Physics of Plasmas **16**, 082105 (2009).

[15] J. Lang, Y. Chen, S. E. Parker, and G.-Y. Fu, Physics of Plasmas **16**, 102101 (2009).

[16] E. M. Bass and R. E. Waltz, Physics of Plasmas **17**, 112319 (2010).

[17] G. Vlad, S. Briguglio, G. Fogaccia, F. Zonca, and M. Schneider, Nuclear Fusion **46**, 1 (2006).

[18] G. Vlad, S. Briguglio, G. Fogaccia, F. Zonca, C. D. Troia, W. Heidbrink, M. V. Zeeland, A. Bierwage, and X. Wang, Nuclear Fusion **49**, 075024 (10pp) (2009).

[19] X. Wang, F. Zonca, and L. Chen, Plasma Physics and Controlled Fusion **52**, 115005 (2010).

[20] B. J. Tobias, I. G. J. Classen, C. W. Domier, W. W. Heidbrink, N. C. Luhmann, R. Nazikian, H. K. Park, D. A. Spong, and M. A. Van Zeeland, Phys. Rev. Lett. **106**, 075003 (2011).

[21] R. B. White, Physics of Fluids B: Plasma Physics **2**, 845 (1990).

[22] B. N. Breizman, H. L. Berk, M. S. Pekker, S. D. Pinches, and S. E. Sharapov, Phys. Plasmas **10**, 3649 (2003).

[23] F. Zonca and L. Chen, Physics of Plasmas **3**, 323 (1996).

[24] C. Z. Cheng and M. S. Chance, Phys. Fluids **29**, 3695 (1986).

[25] M. S. Chu, J. M. Greene, L. L. Lao, A. D. Turnbull, and M. S. Chance, Physics of Fluids B: Plasma Physics **4**, 3713 (1992).

[26] V. Hernandez, J. E. Roman, and V. Vidal, ACM Transactions on Mathematical Software **31**, 351 (2005).